

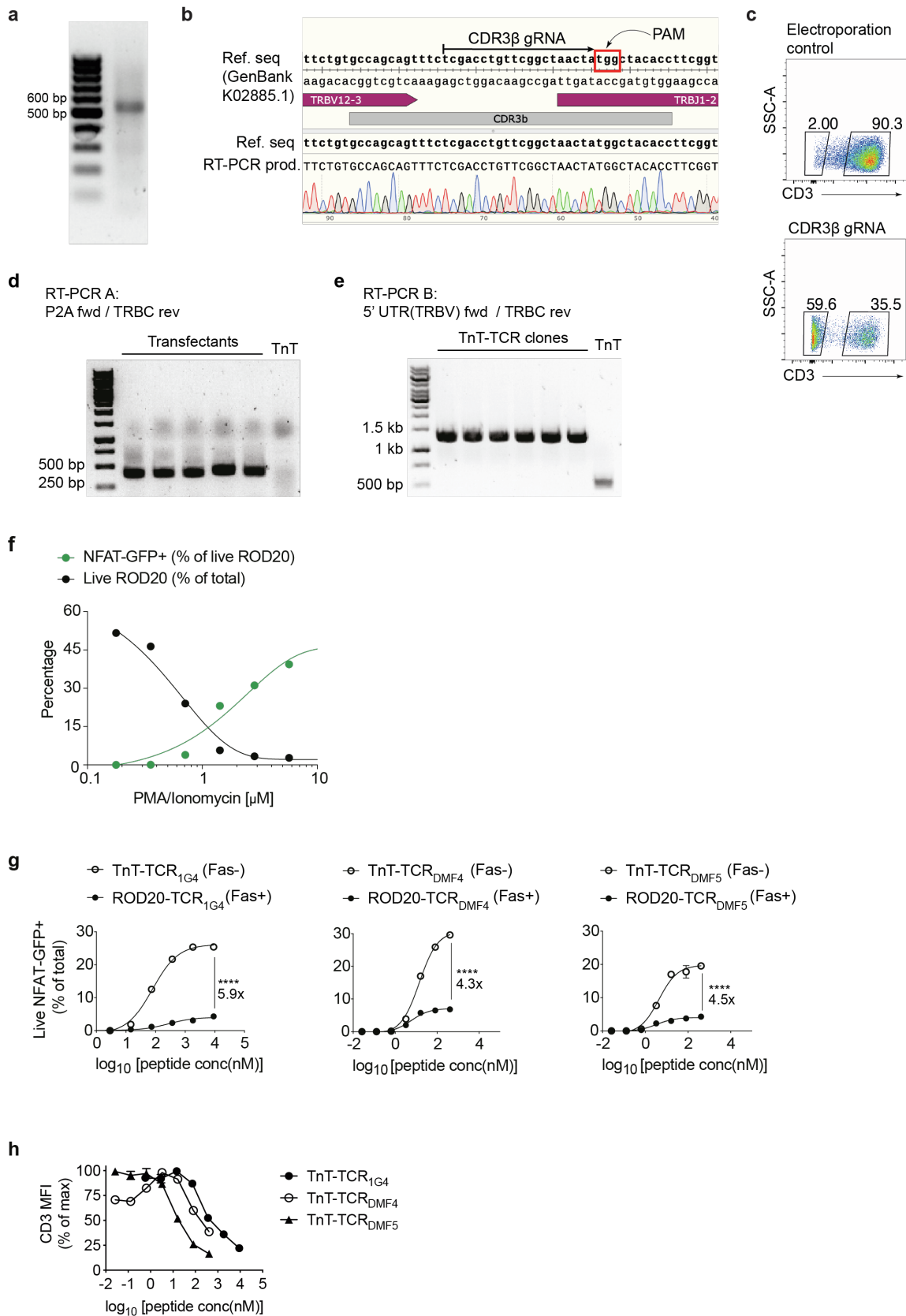
Supplemental information

**High-throughput T cell receptor engineering
by functional screening identifies candidates
with enhanced potency and specificity**

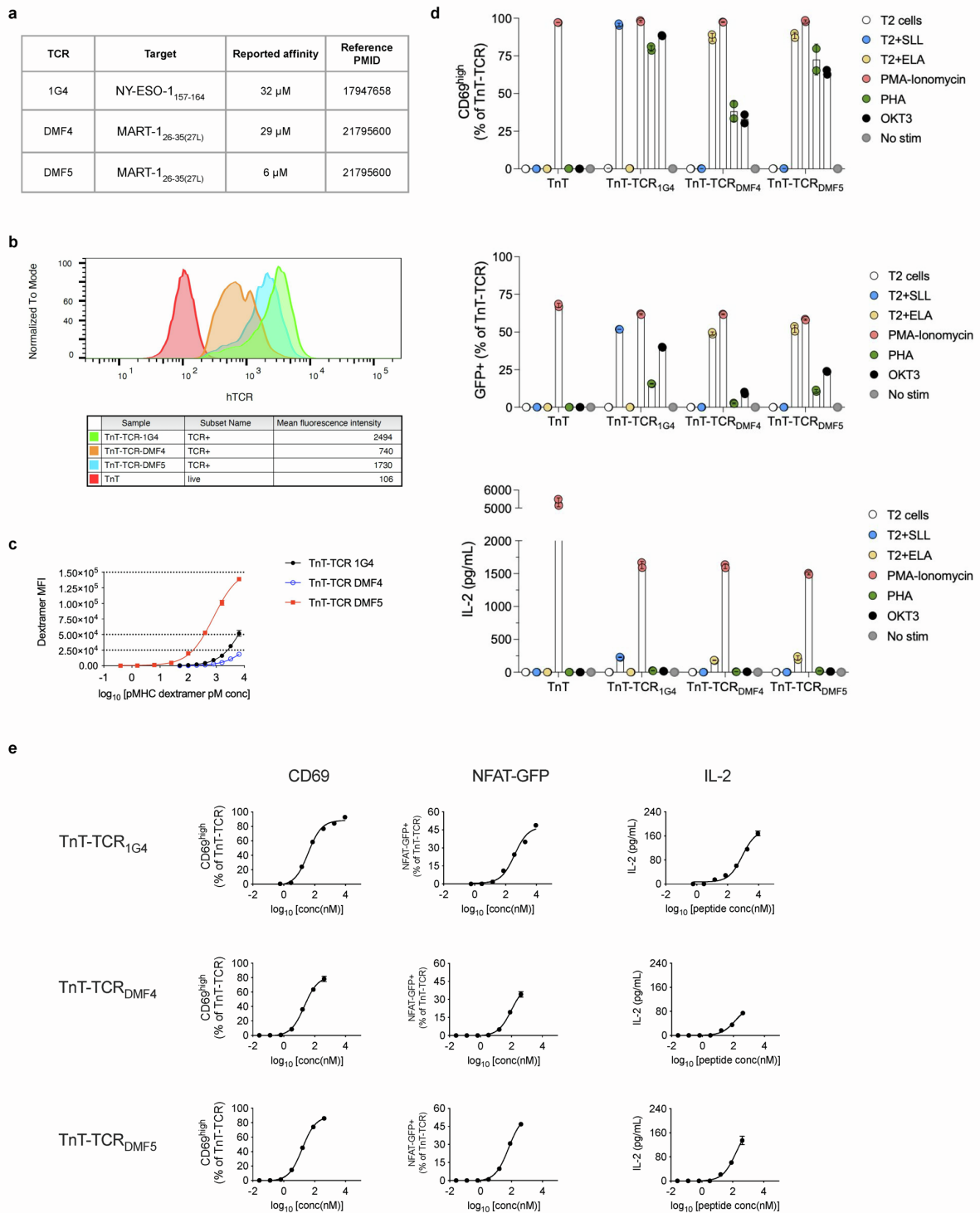
Rodrigo Vazquez-Lombardi, Johanna S. Jung, Fabrice S. Schlatter, Anna Mei, Natalia Rodrigues Mantuano, Florian Bieberich, Kai-Lin Hong, Jakub Kucharczyk, Edo Kapetanovic, Erik Aznauryan, Cédric R. Weber, Alfred Zippelius, Heinz Läubli, and Sai T. Reddy

Supplemental Information

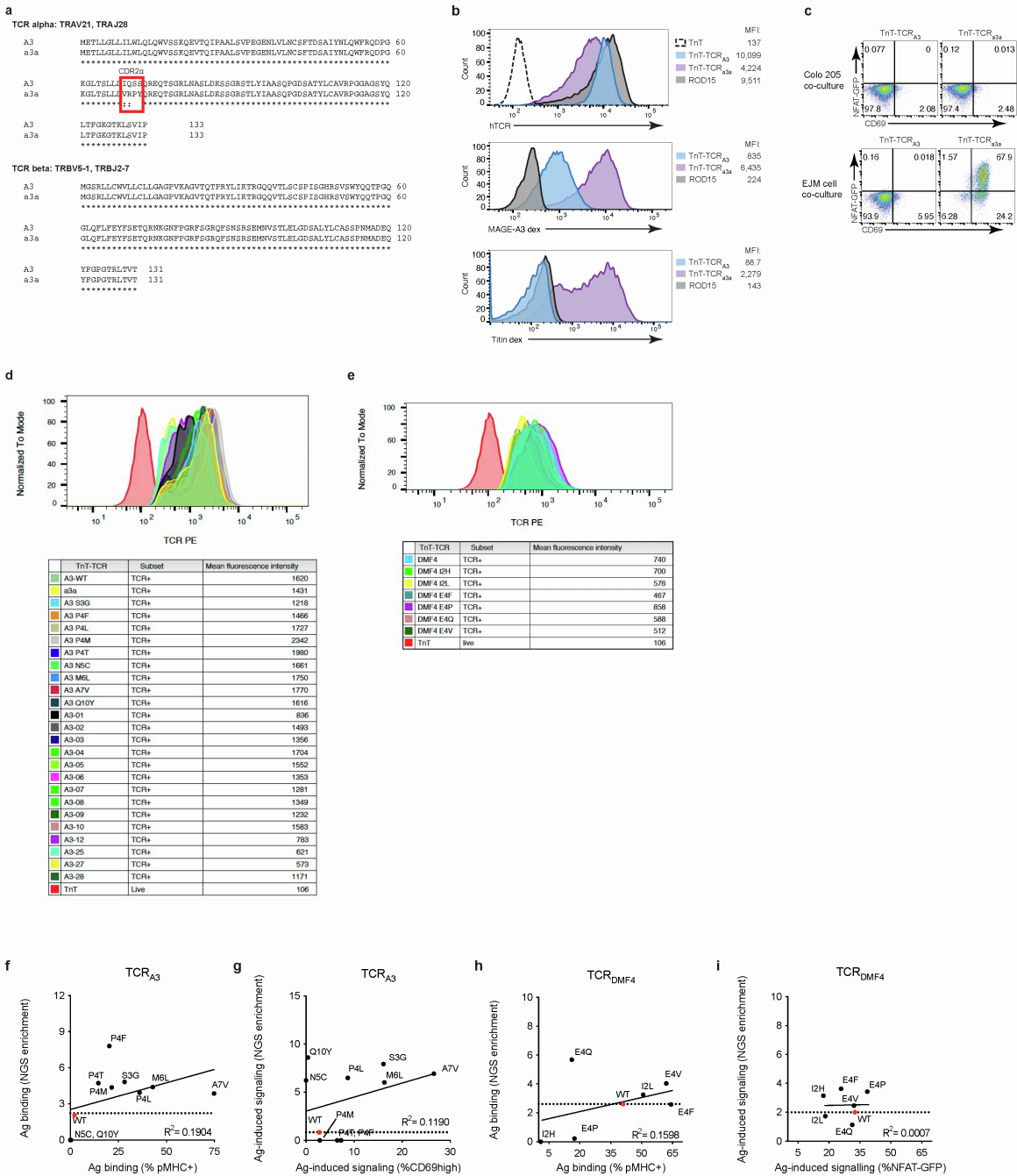
Supplemental Figures 1-7



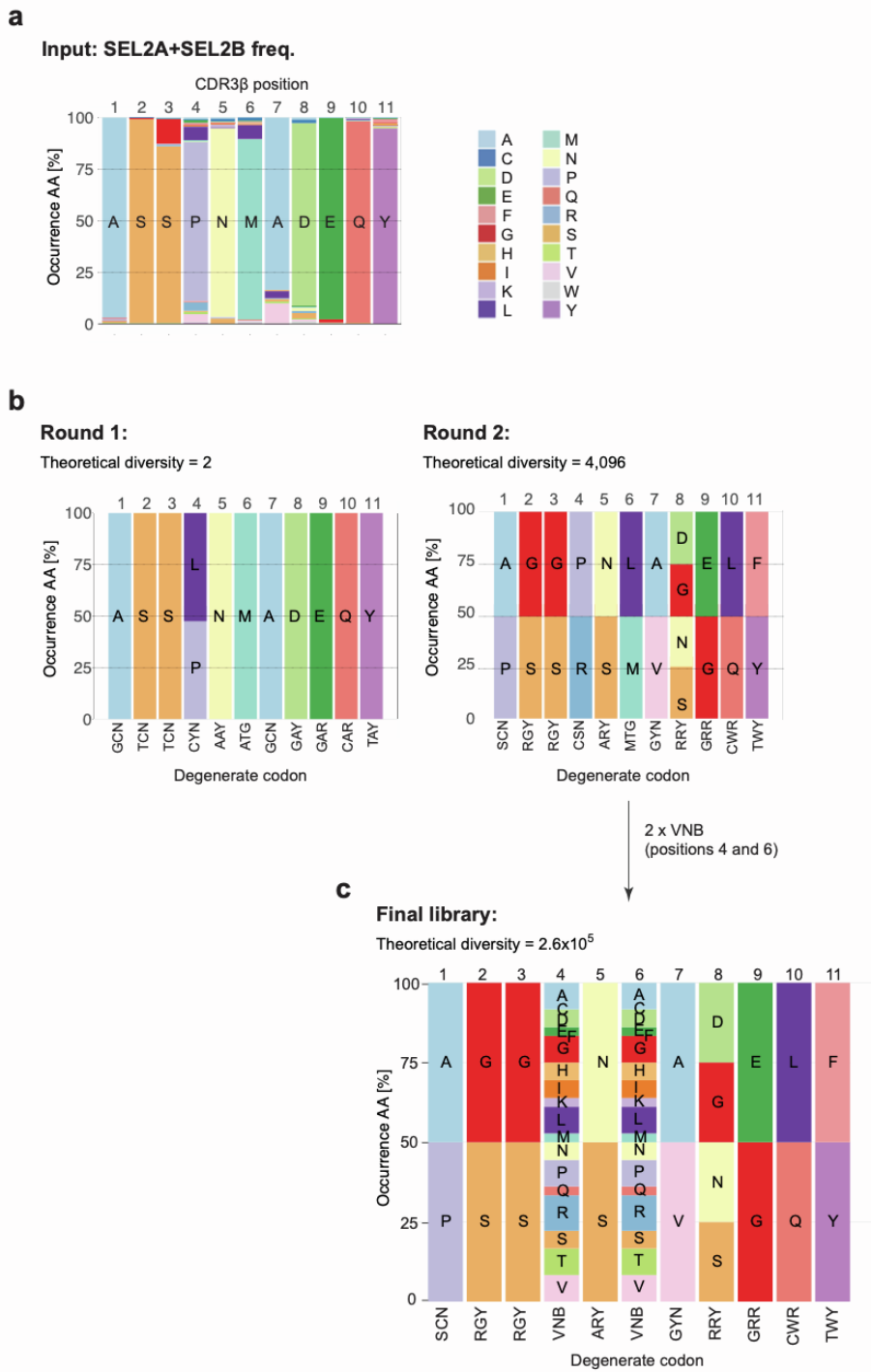
Supplemental Fig. 1. The recombined Jurkat CDR β 3 sequence is an ideal target for monoallelic and physiological CRISPR-Cas9 TCR reconstitution of AICD-resistant TnT cells, Related to Figures 1 and 2. **a**, PCR amplification of TSO-labelled Jurkat cDNA with ISPCR forward and TRBC1/2 reverse (RVL-68) primers. **b**, Sanger sequencing of the ~ 550 bp band in **(a)** confirmed the expression of a single TCR β chain matching the Jurkat TCR β reference sequence (GenBank K02885.1). The designed CDR3 β gRNA is also displayed. **c**, Flow cytometry shows transfection of Cas9+ Jurkat cells with CDR3 β gRNA results in nearly 60% TCR β knockout efficiency, as measured by surface expression of CD3. **d**, Gel shows results of RT-PCR using a forward primer annealing to the P2A sequence within the TCR $\alpha\beta$ HDR template (RVL-144) and a reverse primer annealing to the endogenous Jurkat TRBC (RVL-145). Untransfected TnT cell samples display no PCR product, while samples derived from TCR transfectants display a 435 bp product consistent with targeted TCR integration and correct splicing with TRBC1. Products from RT-PCR were routinely utilized for deep sequencing of TCR selections (Genewiz Amplicon EZ). **e**, Gel shows results of RT-PCR using a forward primer annealing to the 5' UTR of the recombined Jurkat TCR β VDJ exon (RVL-67c) and a reverse primer annealing to the endogenous Jurkat TRBC (RVL-68). Untransfected TnT cells show a 500 bp band corresponding to the endogenous Jurkat TCR β , while TnT-TCR clones display a unique band at 1.3 kb demonstrating targeted integration of TCR $\alpha\beta$ cassettes and their correct splicing with TRBC1 (see Fig.1b). Sanger sequencing of RT-PCR products was routinely performed for clone validation purposes. **f**, Increased cell death in the ROD20 cell line (Cas9+ CD8+ CD4- mRuby+ NFAT-GFP CD3-) after non-specific stimulation with increasing concentrations of PMA-ionomycin. This increase was inversely correlated to the proportion of NFAT-GFP-positive cells within surviving cells, thus indicating that increased cell death resulted from AICD. **g**, TCR $_{1G4}$, TCR $_{DMF4}$ and TCR $_{DMF5}$ were introduced into ROD20 (Fas+) or TnT (Fas-) cells via CRISPR-Cas9 HDR and co-cultured overnight with T2 cells pulsed with serially-diluted target peptides ($n = 2$). Activated TnT-TCR cells displayed significantly higher proportions of live NFAT-GFP-positive cells relative to ROD20-TCR cells, thus indicating confirming resistance to AICD. **h**, CD3 mean fluorescence intensity (MFI) in TnT-TCR cells expressing TCR $_{1G4}$, TCR $_{DMF4}$ or TCR $_{DMF5}$ after co-culture T2 cells pulsed with serially-diluted target peptides ($n = 2$). Non-linear least squares fits and two-way ANOVA with Bonferroni post hoc test for multiple comparisons are displayed in **(f)**, **** $P < 0.0001$. PAM: protospacer adjacent motif. TSO: template-switching oligonucleotide. Experiments were performed once.



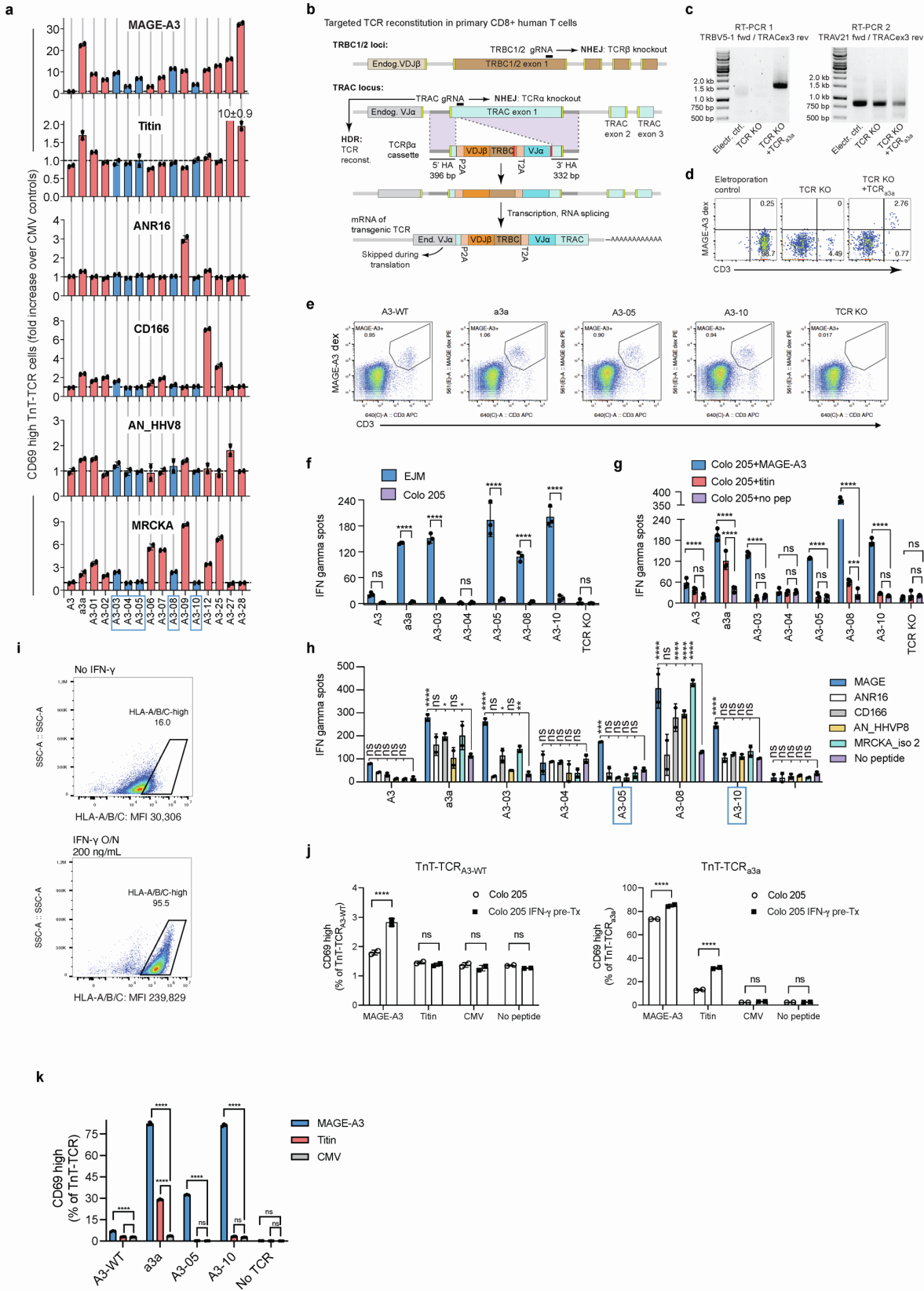
Supplemental Fig. 2. Profiling of TnT-TCR cell activity in response to antigen-dependent and antigen-independent stimulation, Related to Figure 2. **a**, Reported affinity levels of TCR_{1G4}, TCR_{DMF4} and TCR_{DMF5} for their cognate antigens. **b**, Histograms displaying TCR surface expression levels (mean fluorescence intensity) in TnT-TCR cells following CRISPR-targeted reconstitution with TCR_{1G4}, TCR_{DMF4} or TCR_{DMF5}, as assessed by flow cytometry. **c**, Serially diluted target peptide-MHC dextramers were used to assess the binding avidities of TnT-TCR_{1G4}, TnT-TCR_{DMF4} and TnT-TCR_{DMF5} (n = 3). Displayed are the mean fluorescence intensity in the dextramer channel (live TnT-TCR gate) and non-linear least squares fits. **D**, Activation profiling of TnT-TCR_{1G4}, TnT-TCR_{DMF4} and TnT-TCR_{DMF5} following stimulation with soluble PMA/ionomycin, soluble PHA, plate-bound anti-CD3 monoclonal antibody (OKT3), or T2 cells pulsed with NY-ESO-1 (SLL) or MART-1 (ELA) peptides. Shown are the levels of CD69 and NFAT-GFP following stimulation, as assessed by flow cytometry (percent of live TnT-TCR cells), as well as levels of secreted IL-2 as assessed by ELISA (n = 2). **e**, CD69 expression (flow cytometry), NFAT-GFP expression (flow cytometry), and IL-2 secretion (ELISA) levels in TnT-TCR cells after overnight co-culture with T2 cells pulsed with serially diluted cognate peptide (n = 2). Non-linear least squares fits and are shown for each plot. All data are displayed as mean ± SD. Experiments were performed once.



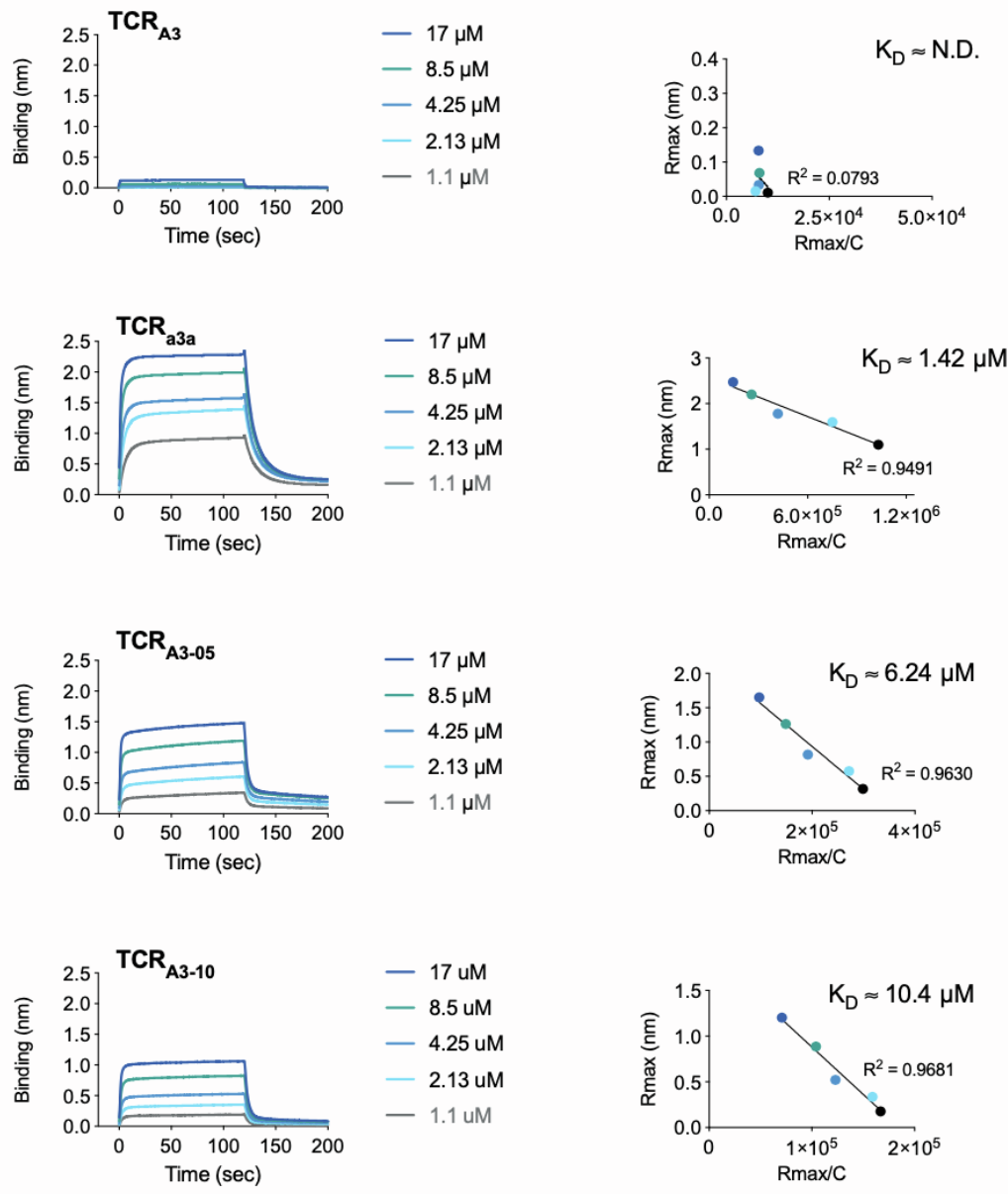
Supplemental Fig. 3. Assessment of TCR expression, antigen binding and antigen-induced signalling in TnT-TCR cells, Related to Figure 3. **a**, Protein sequence alignments of TCR_{A3} and its phage display-engineered variant TCR_{a3a} (WO2012013913). The four substitutions introduced into the CDR2 α of TCR_{a3a} are highlighted in red. **b**, TnT clones expressing TCR_{A3} and TCR_{a3a} were generated by CRISPR-Cas9 HDR followed by single-cell FACS. Levels of TCR expression (anti-TCR monoclonal antibody clone IP26), MAGE-A3 peptide-MHC dextramer binding and titin peptide-MHC dextramer binding in TnT-TCR_{A3}, TnT-TCR_{a3a} and negative control cell lines are displayed. **c**, Flow cytometry of NFAT-GFP and CD69 expression after overnight co-culture of TnT-TCR_{A3} and TnT-TCR_{a3a} cells with Colo 205 (HLA-A*0101 MAGE-A3-) and EJM (HLA-A*0101+ MAGE-A3+) cancer cell lines. **d-e**, Histograms display the levels of TCR surface expression in TnT-TCR transfectants as assessed by flow cytometry. Mean fluorescence intensity levels of (d) TCR_{A3} variants or (e) TCR_{DMF4} variants alongside appropriate positive (i.e., TCR_{a3a}, TCR_{DMF5}) and negative controls (TnT) are displayed. **f-i**, Simple linear regression analyses of deep sequencing enrichment data (**Figs. 3c-d**) and flow cytometry validation data (**Figs. 3e and 3g**) derived from selected TCR_{A3} and TCR_{DMF4} single mutants in terms of antigen binding and antigen-induced signalling. Dotted line represents the wild deep sequencing read enrichment observed for wild-type TCR_{A3} or TCR_{DMF4}.



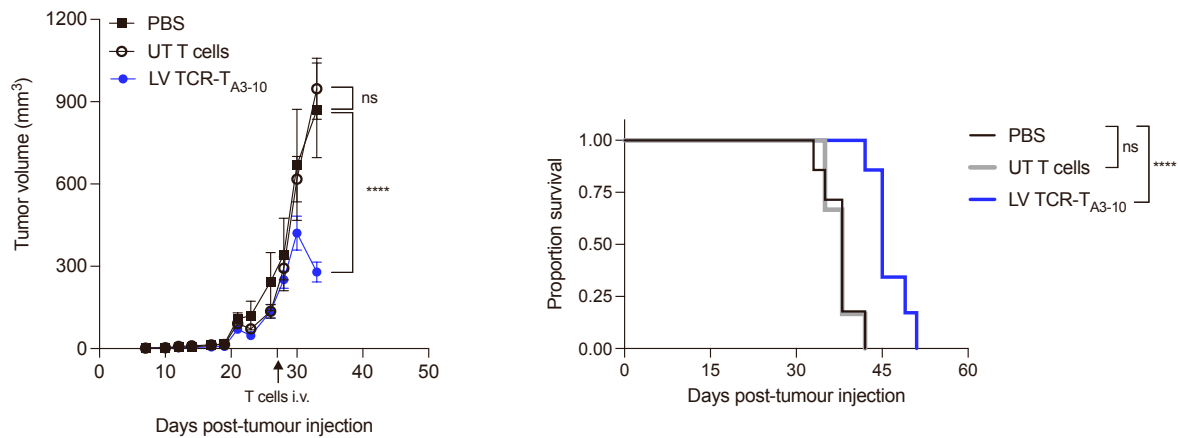
Supplemental Fig. 4. Combinatorial library design based on DMS of the TCR_{A3} CDR3 β , Related to Figure 4. **a**, Bar plots show the frequencies of single mutants present in TCR_{A3} DMS selections 2A (MAGE-A3 peptide-MHC+) and 2B (NFAT-GFP+) (added and normalized to 100%). **b**, Pooled DMS data was used as input for our previously described algorithm (Mason et al. 2018, PMID: 29931269) with the aim of re-capitulating observed amino acid frequencies with degenerate codons (two iterations with varying sensitivity to lower frequency amino acids are displayed). **c**, To take advantage of the full attainable diversity of mammalian cell display, the “Round 2” solution (theoretical diversity of 4,096 sequences) was rationally modified to include two “VNB” codons at positions 4 and 6 (high levels of enrichment in DMS), leading to a theoretical diversity of 2.6×10^5 variants. Degenerate base symbols: R = A, G; Y = C, T; S = G, C; W = A, T; K = G, T; M = A, C; B = C, G, T; D = A, G, T; H = A, C, T; V = A, C, G; N = any base.



Supplemental Fig. 5. TCR-Engine variants display high levels of specificity in TnT cells and primary human T cells, Related to Figure 4. **a**, TnT cells expressing TCR_{A3}, TCR_{a3a} and selected TnT_{A3} variants were co-cultured with Colo 205 cells pulsed with a subset of predicted off-target peptides. The percentages of CD69^{high} TnT-TCR cells were determined by flow cytometry and normalized to their respective CMV backgrounds (n = 2). Selected TnT-TCR_{A3} variants displaying favorable cross-reactivity profiles are highlighted in blue. **b-e**, CRISPR-targeted reconstitution of primary human CD8+ T cells with transgenic TCRs. **b**, Adapted CRISPR-Cas9-based method for dual knockout of endogenous TCRα and TCRβ chains and simultaneous reconstitution with transgenic TCRs targeted to the TRAC locus (see also STAR Methods). The lack of a complete TRAC region in the designed TCRβ_a HDR templates made splicing with endogenous TRAC exons a requirement for transgenic TCR surface expression. Regions highlighted in red were recoded in order to prevent targeting of HDR templates. Transgenic TCR expression is dependent on correct RNA splicing with endogenous TRAC exons 2 and 3. **c-d**, Validation of the approach is shown for TCR_{a3a}. **c**, RT-PCR with a forward primer annealing to the transgenic TRBV5-1 gene and a reverse primer annealing to the endogenous TRAC exon 3. Electroporation control and dual TCR knockout samples display no PCR product, while samples derived from TCR_{a3a} transfecants display a 1.6 kb product consistent with targeted TCR integration and correct splicing with endogenous TRAC. A second RT-PCR reaction amplifying both endogenous and transgenic TRAV21-TRAC TCRs is shown as a positive control. **d**, Flow cytometric assessment of CD3 expression and MAGE-A3 peptide-MHC dextramer binding in primary CD8+ T cells reconstituted with TCR_{a3a}. **e**, Flow cytometric assessment of CD3 expression and MAGE-A3 peptide-MHC dextramer binding in primary CD8+ T cells reconstituted with TCR_{a3a}. **f-g**, Example CRISPR-targeted TCR reconstitution experiment showing expression of TCR_{A3}, TCR_{a3a}, TCR_{A3-05}, TCR_{A3-10} in edited primary human CD8+ T cells, as determined by flow cytometry (n = 1). **f-g**, Functional assessment of selected TCR_{A3} variants expressed on the surface primary human CD8+ T cells, as measured by IFN-γ ELISpot. Primary human CD8+ T cells were transfected with Cas9 RNP complexes targeting the TRAC and TRBC regions, along with TCR-encoding HDR templates. A no-HDR-template control (TCR KO) was also included. **f**, Activation of edited CD8+ T cells following co-culture with MAGE-A3-positive EJM cells or MAGE-A3-negative Colo 205 cells (n = 3). 5x10⁴ T cell transfectants plus 1.5x10⁴ EJM or Colo 205 cells per well. **g**, Activation of edited CD8+ T cells following overnight co-culture with Colo 205 cells pulsed with MAGE-A3, titin, or no peptide (n = 3). 4x10⁵ T cell transfectants plus 1.5x10⁴ Colo 205 cells per well. **h**, Activation of edited CD8+ T cells following overnight co-culture with Colo 205 cells pulsed with a panel of potential off-target peptides (n = 2). 2.5x10⁵ T cell transfectants plus 1.5x10⁴ Colo 205 cells per well. Blue boxes highlight variants TCR_{A3-05} and TCR_{A3-10}, which display negligible cross-reactivity. **i**, Overnight stimulation of Colo 205 with 200 ng mL⁻¹ human IFN-γ results in a 8-fold increase in mean fluorescence intensity of surface HLA class I expression. **j**, Overnight stimulation of Colo 205 with 200 ng mL⁻¹ human IFN-γ significantly enhances the sensitivity of TnT-TCR cells to pulsed peptides (n = 2). **k**, Assessment of TnT-TCR activation in response to peptide-pulsed Colo 205 cells pre-treated with IFN-γ, as measured by flow cytometry detection of CD69 expression, reveals a lack of cross-reactivity to titin by TCR_{A3-05} and TCR_{A3-10} (n = 3). Asterisks indicate significant differences between indicated groups as determined by two-way ANOVA with Bonferroni post-hoc test for multiple comparisons. Data are displayed as mean ± SD. * P < 0.05, ** P < 0.01, *** P < 0.001, **** P < 0.0001, ns = not significant. Experiments were performed once.



Supplemental Fig. 6. TCR-Engine variants display enhanced binding affinity to MAGE-A3 pMHC, Related to Figure 6. Biolayer interferometry analyses of soluble TCR binding to immobilized MAGE-A3 HLA-A*0101 monomers. K_D values were approximated by Scatchard analyses of R_{max} vs. $R_{\text{max}}/\text{concentration}$ plots (K_D in molar \approx negative of linear regression slope).



Supplemental Fig. 7. LV TCR-T_{A3-10} cells mediate tumor regression and prolonged survival of NSG mice harboring established A375 melanoma tumors, Related to Figure 7. The antitumor activity of LV TCR-T_{A3-10} cells was assessed in a xenogeneic A375 melanoma mouse tumor model. NSG mice were injected s.c. in their left flanks with 5×10^6 A375luc2 cells on day 0 ($n = 6$), followed by treatment with a single i.v. dose of PBS, 1×10^7 UT T cells or 1×10^7 TCR-T_{A3-10} T cells on day 27. All mice (including those in the PBS group) were injected periodically with s.c. injections of recombinant human IL-2 (2.75 μ g per dose) in order to promote T cell engraftment (dosing schedule described in methods section). Following treatment, mice were monitored for tumor growth (left panel) and survival (right panel). Data are displayed as mean \pm SEM. Mouse survival (right panel) is displayed using Kaplan–Meier plots and compared by the log-rank (Mantel-Cox) test. Asterisks indicate significant differences as determined by two-way ANOVA with Bonferroni post hoc test for multiple comparisons. * $P < 0.05$, ** $P < 0.01$, *** $P < 0.001$, **** $P < 0.0001$, ns = not significant. Experiment was performed once.

Supplemental Tables 1-6

Supplemental Table 1. Previously discovered TCRs and target peptides utilized in this study, Related to Figures 2 and 3.

Name	Target protein(s)	Target peptide	MHC restriction	Peptide sequence	Comments
TCR _{1G4}	NY-ESO-1	NY-ESO-1 ₁₅₇₋₁₆₄	HLA-A*0201	SLLMWITQC	
TCR _{DMF4}	MART-1	MART-1 _{26-35(27L)}	HLA-A*0201	E <u>L</u> AGIGILTV	Anchor-modified peptide
TCR _{DMF5}	MART-1	MART-1 _{26-35(27L)}	HLA-A*0201	E <u>L</u> AGIGILTV	Anchor-modified peptide
TCR _{A3}	MAGE-A3	MAGE-A3 ₁₆₈₋₁₇₆	HLA-A*0101	EVDPIGHLY	
TCR _{a3a}	MAGE-A3 Titin	MAGE-A3 ₁₆₈₋₁₇₆	HLA-A*0101	EVDPIGHLY	
		Titin _{24,337-24,345}	HLA-A*0101	ESDPIVAQY	

Supplemental Table 2. Unique clones identified in SEL 3A (MAGE-A3-induced signalling) and SEL 3B (titin-induced signalling) by means of deep sequencing, Related to Figure 4.

Total clones SEL 3A + 3B	Clones in SEL 3A only	Clones in SEL 3B only	Clones in both SEL 3A and SEL 3B	Clones enriched >2-fold in SEL 3A and not enriched in SEL 3B (enrich. over SEL 1)
1600	910	365	325	195

Supplemental Table 3. Top-ranked TCR_{A3} variants with predicted high specificity for MAGE-A3, Related to Figure 4. Experimentally validated variants are highlighted in bold.

TCR	SEL 2 (MAGE) enrichment over SEL 1	SEL 3A (MAGE) enrichment over SEL 1	SEL 3B (titin) enrichment over SEL 1	SEL 3A frequency rank	SEL 3A enrichment rank	Score
A3-001	41.9	130.5	0.0	45	8	53
A3-002	54.8	103.1	0.0	59	13	72
A3-003	53.1	78.2	0.0	76	19	95
A3-004	82.1	78.1	0.0	77	20	97
A3-005	25.9	65.7	0.0	21	24	45
A3-006	71.7	65.6	0.0	89	25	114
A3-007	43.5	63.3	0.0	93	26	119
A3-008	35.4	57.0	0.0	97	31	128
A3-009	32.2	55.9	0.0	99	33	132
A3-010	88.6	53.5	0.0	102	34	136
A3-011	19.1	48.9	0.0	31	40	71
A3-012	25.0	46.0	0.4	8	45	53
A3-013	39.5	43.4	0.0	124	50	174
A3-014	23.4	42.2	0.0	127	53	180
A3-015	20.9	41.0	0.0	132	55	187
A3-016	33.8	41.0	0.0	133	56	189
A3-017	26.1	40.4	0.0	70	58	128
A3-018	35.6	39.1	0.0	40	60	100
A3-019	29.0	38.5	0.0	136	61	197
A3-020	25.8	37.3	0.0	139	63	202
A3-021	26.1	34.7	0.0	83	68	151
A3-022	24.5	33.5	0.0	43	74	117
A3-023	9.2	31.6	0.0	92	76	168
A3-024	11.4	22.1	0.0	41	98	139
A3-025	12.1	21.8	0.5	88	99	187
A3-026	15.8	19.3	0.0	62	110	172
A3-027	4.9	17.9	0.2	50	117	167
A3-028	13.6	15.4	1.0	11	133	144
A3-029	10.3	15.4	0.1	29	134	163

Supplemental Table 4. List of candidate off-target peptides shared by TCR_{a3a}, TCR_{A3-05} and TCR_{A3-10}, as predicted from peptide scanning of the MAGE-A3₁₆₈₋₁₇₆ target using TnT-TCR cells as effectors, Related to Figure 6.

Pep No.	Protein	Start position	End position	Sequence	Pep No.	Protein	Start position	End position	Sequence	Pep No.	Protein	Start position	End position	Sequence	Pep No.	Protein	Start position	End position	Sequence	Pep No.	Protein	Start position	End position	Sequence	Pep No.	Protein	Start position	End position	Sequence
1	5HT2A	243	251	EIPIPLTMV	61	CHSTE	362	370	FAYPLPNVT	121	FNDC8	287	295	ENYPIQITV	181	MAGI1	540	548	QSIPFAGSV	241	PKL2	367	375	FGDPLWIVQ	301	TFFC	282	290	FSDPPLSYTF
2	A16L2	497	505	QVIPVGGRV	62	CLD15	146	154	FFDPLVPGT	122	FRIL6	977	985	QIVPV PANI	182	MARE1	234	242	ENDPVLQRI	242	PLD5	387	395	ETDPLTNRF	302	THIL	234	242	EVIPVTVT
3	A1CF	71	79	EIPLCEKI	63	CND2	240	248	EIDPMFOKT	123	FSO1L	201	209	EIDPVEELV	183	MED6	91	99	QVIPLAGDT	243	PP1R8	107	115	QQIPIDSTV	303	TIF1A	924	932	FQDPVPLTC
4	AAK1	917	925	EIDPVPVL	64	CNOT1	710	718	QIDPLAGMT	124	GATA1	76	84	QVYPLLNCM	184	MEF6	319	327	EGDPLVDGTC	244	PPM1H	298	306	EQIPMSSEF	304	TIGIT	138	146	FQIPLLGAM
5	ABCAC	531	539	QIPLIEAM	65	CNOT4	377	385	EIPIVSSST	125	GBG5	44	52	QHDPLLTGV	185	MGST2	58	66	EYFPIFIT	245	PR14L	705	713	QTIPQTKI	305	TITIN	2437	2443	ESPDIVAGY
6	ABCAC	858	866	QAPIMLQNT	66	CNOT5	162	170	EIPICLRL	126	GFP72	217	225	EQIPILYRT	186	MNDA	208	216	QNDPVTVVV	246	PRC2B	1957	1965	QQIPISLHT	306	TKFC	128	136	EGIPVEMMV
7	ABCAC	357	365	EVDPIEHT	67	CNTN2	524	532	QHPPLLDII	127	GLT16	270	278	EQIPLEKHM	187	MOC51	549	557	QLIPLHHV	247	PRD16	862	870	FDPIYLSRV	307	TML1	446	454	EDPPLAPAV
8	ABEC4	259	267	ESYPLINAF	68	COG6	1892	1900	EIIPVVITF	128	GPR18	196	204	FIPLFLIMI	188	M0D5	85	93	FVDFLVNTY	248	PRDM6	184	192	EIPLNQHT	308	TMW2	539	547	FNIPLMAYM
9	ACACA	2174	2182	EIPIYHQV	69	CG04	351	359	EIDLPITEV	129	GRHL3	257	265	QPVYPLTFT	189	MORC1	570	578	QFIPDEIT	249	PRDX1	42	50	FFYPLDFTF	309	TPC11	993	1001	ENIPVTTV
10	ACADM	59	67	EIPVAAEY	70	COQ5	265	273	EIPIVPLGEV	130	GRIA1	531	539	FLDPLAYEI	190	MROH8	70	78	QQDPLSEAI	250	PR510	114	122	EVDPLVYNN	310	TR49B	22	30	FDPPVTDTC
11	AQL7A	231	239	EYGPLPSIT	71	CP2A6	390	398	EVYPMLGSV	131	GST2	110	118	FGIPLWVQV	191	MTFR2	56	64	ELIPLLNSV	251	PTPRB	1131	1139	QVDPVLQSF	311	TR64C	22	30	FDPPVTDTC
12	AEBP1	916	924	QIPIRANAT	72	CP3A5	215	223	EIPLPLSII	132	GTC1	51	59	QTIPSEHY	192	MXR45	1804	1812	ONIPMVSST	252	PUR4	92	100	EMIPREVWC	312	TR11	23	31	FTDPVMTDC
13	AFAD	1217	1225	EAYPIPQT	73	CPED1	371	379	FMPYVPLQV	133	HACD3	299	307	QSIPIINET	193	MXRA5	2544	2552	FHDPISEKI	253	RAS4B	289	297	QLIPLIQET	313	TR117	23	31	FTDPVMTDC
14	AGRE4	300	308	FMYPVGYGI	74	CPLH1	363	371	EIPLHPLU	134	HDC4	996	1004	EDPLPKEV	194	MY15B	737	745	EAIPLAPGI	254	RBBP6	365	373	QDDPLMPV	314	TR41	27	35	FTDPVSIQC
15	AGR66	716	724	QVDPPLASV	75	CPLN1	2416	2424	QDPLNLII	135	HD	2801	2809	QLIPVPSDY	195	MYBB	388	396	EIPLSPST	255	RBM25	753	761	FAYPLDWSI	315	TR51	22	30	FLDPVTDTC
16	AGR1L	42	50	EYGPIELRL	76	CRBG2	1635	1643	EVPPMMPEV	136	HELQ	1009	1017	EIPLMEVT	196	MYO1H	174	182	QGIPVFVGH	256	RPB1	190	198	FGIPLADAV	316	TR58	267	275	ENIPMLEKT
17	AGR3L	37	45	ESYPIELRC	77	CRBG3	1706	1714	EIPIVPLAM	137	HELZ2	612	620	TDQTPVTLQY	197	MYO2Z	242	250	ENIPVIFTT	257	RELCH	541	549	EULIPILCT	317	TRM4	19	27	FQDPVSIEC
18	ALPK3	1702	1710	EIPILYLIY	78	CRBN	79	87	EIPIVPLQV	138	HERC1	4283	4281	QCIPLVLAGV	198	NCHL1	145	153	EGDPIVLP	258	RELN	1226	1234	QVIPVINP	318	TRIO	2687	2695	FVPLSEVT
19	AMPE	711	719	EIPLMEEY	79	CSD01	279	287	QNDPLPGRI	139	HERC1	4647	4655	EMPLDSFV	199	NELF0	571	579	EHDPIVTERI	259	REV3L	2317	2325	EDPFLCAFL	319	TSH1	466	474	QSLPLPPTT
20	AN13A	377	385	QVPIPHDLM	80	CSKP	767	775	EIAYPIHPT	140	HEXD	82	90	EIPLVQTF	200	NEMF	388	396	QGDPPVASAI	260	RFIP3	118	126	ELDPPLSWT	320	TSH1	95	103	FSYPLVASC
21	AN08	980	988	QIPILOGKF	81	CSPG2	1360	1368	EIDPVHDL	141	HMHCN1	994	1002	EIPIVPLPC	201	NEMF	995	1003	FAPICAPY	261	RGP24	1369	1377	EULPTARM	321	TT21A	441	449	OQIPLGSEY
22	ANR16	147	155	EGDPLILQY	82	CTR4	540	548	EIQIPMVPV	142	HNRC1	250	258	EQDPLDDDV	202	NEP1	178	186	FSIPIVPSDV	262	RHAG	49	57	EYPLPQDFV	322	TT30A	438	446	ENYPMVEKV
23	ARM6D	143	151	QFIPPLTRT	83	CWC22	121	129	EIPLPLTRT	143	HRH3	86	94	EIPIVPLPV	203	NFE2	178	182	EMYPPVEY	263	RP1R1	720	728	QADPMAPRT	323	TT30B	438	446	ENYPMVEKV
24	ARRD1	328	336	FIDPVFLST	84	DDX1	56	64	EISIPVQIV	144	HFS2	259	267	ENIPVIEPT	204	NPF2	169	177	EYFPVPPY	264	RM11	62	70	EQIPLPTK1	324	TTC14	535	543	ECYPLVANT
25	ARRD2	199	207	EIVIPVFAEI	85	DDX23	445	453	EIPLVLLVI	145	HSP7E	365	373	EVPIGAII	205	NLGNX	497	505	FGIPMIGPT	265	RM40	81	89	EUIPEOFI	325	TTL2	176	184	QFIPLTVF
26	ARRD4	210	218	EIPIYAEI	86	DDX24	247	255	EIPIMHAV	146	IDD	43	51	QCIPLWPQG	206	NMES1	121	20	EIPLVVF	266	RNF37	263	271	FLDPLTLEI	326	TFW2	246	254	EGDPLPLESV
27	ARSGD	18	26	EFLYPLDF	87	DDX46	224	232	EIDPLVADYM	147	IFNA2	74	82	EIPIVHEM	207	NOX3	397	405	FHYPLVFCVC	267	RP1	1070	1078	ODPIEET	327	TX13C	154	162	QVYPMODF
28	ASHL1	2748	2756	EIPILEAVV	88	DEN6B	427	435	EIPILEHYM	148	GSF2	35	43	EYGPYVSGC	208	NPBW1	212	220	FAIPVSTIC	268	RPB2	86	94	ETDPLIAMI	328	UBE2W	76	84	ENIPVPHV
29	AT11B	351	359	EIPIYLVV	89	DHK9	1123	1131	EIDPVPNERM	149	GSF3	159	167	EQDPLLETC	209	NTRK2	609	617	EGDPLIMV	269	RRBP1	1284	1292	QDIPVOLKT	329	UBP38	242	250	QHIPLOMPT
30	AT11C	356	364	EIPIVSMYV	90	DIPI2A	1561	1569	EIPLPVAY	150	L7RA	237	245	EMDPLILLT	210	NUPBL	197	205	QNIPRTGAV	270	RSH4A	527	535	EIPVPLVELV	330	UBP8	658	666	FLDPLTGTF
31	AT13A	544	552	QGDPLDKM	91	DIPI2B	426	434	EIVIPVIEV	151	IQN	341	349	QTYPVWSVT	211	NUMB	509	517	SGYPVANGM	271	RUSD2	494	502	ETDPLCAEC	331	URAS1	24	32	FLIPVALR
32	ATP7A	660	668	EIPIVGMGL	92	DLG1	822	830	EIPLVSI	152	LBFB6	393	401	QIPLVVARM	212	OS1A7	27	35	EISIPCLMY	272	S12A3	487	495	OLYPLGF	332	UTP20	236	234	EIPPLCLMT
33	ATP7B	660	668	EIPIVMAJM	93	DLG2	788	796	EIPLIAIFI	153	ITAB8	1008	1016	EISIPLWVII	213	ODAM	107	115	QVDPLOLOT	273	S15A1	10	18	FGYPLSIFF	333	VAFNB	57	59	EMYPVPPIT
34	B3A3	930	938	EIPLISILV	94	DLGP1	61	69	EISDPLASST	154	ITBT7	148	156	EYGPYDLYY	214	OMA1	510	518	EIPLTIVY	274	S6A20	117	125	QDQPLPWV	334	VATA	417	425	FSDPVLSVT
35	B3GN7	321	329	EIPLDDDF	95	DNA13	38	46	EIPLVLT	155	JAK2	34	42	QIPLVLOVY	215	OPLA	732	740	QDPLQSLI	275	SCAF4	349	357	QDQPMHQQV	335	VDLR	126	134	QCPVLSWR
36	B3GN8	64	72	EIPLPFAV	96	DND1	73	81	EIPLQFQRV	156	JIP14	919	927	FTDPLGVQI	216	OPRK	238	243	FVIPVLLIII	276	SCAM1	256	264	QNIPVGIMM	336	WB5B1	49	57	FVYPLDECT
37	BCL7C	179	187	EAYPVPEV	97	DSCAM	714	722	EIPIVPTV	157	K1210	525	533	QGYPMSAA	217	OPSD	212	220	EIPLMIFL	277	SCAP1	284	292	EIPLVTTT	337	WASH1	188	196	FLDPLAGAV
38	BDH	225	233	EIPLGVKV	98	DUS18	82	90	EFDPIADH	158	K154L	1245	1253	EIPLVQET	218	OR1G1	23	31	EIPLRFLV	278	SCN1A	788	796	EHYMPDHF	338	WDFY4	313	321	EYGPLLKV
39	BEND1	348	356	EISIPVQCT	99	DUS21	84	92	EFDPIADU	159	KALRN	2853	2861	EIPLVPLSGT	219	OR2J1	252	252	EIPLVMCMY	279	SCN2A	779	787	EHYMPTEQF	339	WDR27	491	499	EAYPVCEAV
40	BRWD3	1007	1015	EIDPLSGKM	100	DYH11	3798	3806	EIDPLLEDF	160	KCNK1	139	147	EIPLMFLV	220	RSK4	202	210	FSIPIQIFT	280	SCN4A	598	606	EHYPTEHF	340	WFS1	343	351	FFPLVLLT
41	BUD13	541	549	EIDPMANP	101	DYH7	836	844	EIPLQIV	161	KDM2A	303	311	EIPLMQLK	221	OR6K6	55	63	EIPLLIIY	281	SCNNA	110	118	FSYPLVSLNI	341	XPO2	40	48	ONPLPLLLT
42	C10L1																												

Supplemental Table 5. HLA-typed B-LCL lines used for alloreactivity screening (European Collection of Authenticated Cell Cultures, ECACC), Related to Figure 6.

B-LCL	HLA-A		HLA-B		HLA-C	
B-LCL 88	3	24	13	62	6	-
B-LCL 133	1	2	8	60	3	7
B-LCL 220	25	11	14	18	5	8
31708	2301	6802	1503	35	0202	0401
JS	3003	0301	0702	1801	0501	0702
B-LCL 129	1	3	7	8	7	-

Supplemental Table 6. Sequences of DNA oligonucleotides utilized in this study, Related to STAR Methods.

Purpose	Oligo name	Sequence 5'-3'	Annealing temp (°C)
CD8 α -P2A-CD8 β PCR	RVL-50	cgtacaggatccgtatggccttaccagtgaccgc	72
	RVL-51	tgc当地caacgcgtactgtcactaagatacattgtatggttgg	
CD4 PCR	RVL-101	gatgttggacggcgataatggaa	65
	RVL-102	tgtggagctaggcaacaagaa	
Labeling of cDNA 3' ends	TSO	AAGCAGTGGTATCAACGCAGAGTGAATrGrG+G	n/a
Jurkat TCR α template-switching RT-PCR	ISPCR	aaggcagtgttatcaacgcagagt	64
	RVL-70	tctcagctgttacacggcag	
Jurkat TCR β template-switching RT-PCR	ISPCR	aaggcagtgttatcaacgcagagt	62
	RVL-68	agatctctgttctgtatggcctc	
Jurkat TCR α RT-PCR	RVL-69	cagtccgtgacccagcttgg	62
	RVL-70	tctcagctgttacacggcag	
NFAT-GFP HDR template generation (AAVS1)	RVL-119	tgctttctgtaccaggattctctc	72
	RVL-120	agagcagagccaggaaccc	
AAVS1 PCR 1	RVL-137	cacctactcagacaatgcgtatgc	60
	RVL-138	gaactctgcctctaacgcgtc	
AAVS1 PCR 2	RVL-139	ctgggataccccaagagtgagt	65
	RVL-140	ccgcctggaaagggttagagggaaa	
TnT-TCR PCR	RVL-71	gtgccctctcttttgttgc	61.5
	RVL-72	gattcaggcagagggtggagtt	
TnT-TCR RT-PCR A (amplicon for deep seq.)	RVL-144	gaggagaacccctggacctatg	60
	RVL-145	ggaacacccgttgcaggctc	
TnT-TCR RT-PCR B	RVL-67c	ttcttgctcatgctcacagagg	62
	RVL-68	agatctctgttctgtatggcctc	
Plasmid library PCR (amplicon for deep seq.)	RVL-144	gaggagaacccctggacctatg	66
	RVL-154	ctagagacccccagccttacc	
Primary T cell RT-PCR 1	TRBV5-1_fwd	atccctggtaccaacagaccccaggacag	68
	TRACex3_rev1	gtcatgagcagattaaacccggccac	
Primary T cell RT-PCR 2	TRAV21_fwd	atggaaaccccttgggcctg	62.3
	TRACex3_rev2	aaacccggccactttcag	
TCR $\alpha\beta$ HDR template generation (TnT cells)	RVL-127	gcatgcctctgtccaaacag	70
	RVL-128	tttatctgtcatggccgtgacccg	
TCR $\beta\alpha$ HDR template generation (1° T cells)	RVL-166	ctgcctttactctgtccagagttatattgc	62
	RVL-167	gacatcatgaccagagctctgg	
Nicking mutagenesis TCR α DMS	A3_NNK1	ggccctttatcttgcnkagcagccgaatatggcg	n/a
	A3_NNK2	ggccctttatcttggtgcnnkagccgaatatggcgatgaaca	
	A3_NNK3	ggccctttatcttggtgcnnkccgaatatggcgatgaaca	
	A3_NNK4	ggccctttatcttggtgcnnkkaatatggcgatgaacagtc	
	A3_NNK5	ggccctttatcttggtgcnnkgnkagccgatgaacagtac	
	A3_NNK6	tcttgcgcacgcggcaatnnkgcggatgaacagtac	
	A3_NNK7	cgccacgcggcaattnkgcggatgaacagtactcg	
	A3_NNK8	gcagcccaatatggcnnkgaacagtactcg	
	A3_NNK9	cgaatatggcggatnkcgtactttggccggcaccagg	
	A3_NNK10	gaatatggcggatgaannktactcggccggcaccaggctc	
	A3_NNK11	atatggcggatgaacagnnkttcgccggccggcaccaggctc	
Nicking mutagenesis TCR α DMS	DMF4_NNK1	cagacatctgtgtactctgtgnkcatcgtggatgggttggg	n/a
	DMF4_NNK2	atctgtgtactctgtgcnnkagtggatgggttggg	
	DMF4_NNK3	gtgtactctgtgcnnkagtggatgggttggg	
	DMF4_NNK4	tacttctgtgcnnkagtggatgggttggg	
	DMF4_NNK5	ctgtgcnnkagtggatgggttggg	
	DMF4_NNK6	gtgcnnkagtggatgggttggg	
	DMF4_NNK7	ccatcgtggatgggttggg	
	DMF4_NNK8	tgtgcnnkagtggatgggttggg	
	DMF4_NNK9	cagtggatgggttggg	

DMF4_NNK10	gaggtaggggtgggcagnnkcgacatttgtatggg		
DMF4_NNK11	gttaggggtggcagccnnkcattttgtatgggact		
DMF4_NNK12	gggtgggcagccccagnnktttgtatggactcg		
Nicking mutagenesis (2nd strand synthesis)	RVL-128	tttatctgtcatggccgtgaccg	n/a
Combinatorial TCR _{A3} library OE-PCR	A3_fwd_ultramer	atcctgttaccaacagaccccaggacaggccctcagtccctttgaa tacttcagtgagacacagagaacaaaggaaactccctggtcattc tcaggccgcaggctctaactctcgctctgagatgaatgtgagcacctt ggagct	70
	A3_rev_ultramer	taggctctccatagagaccccccagccttacctgtgaccgtgagcctggtg cccgcccaarwaywgyccryynrcvnbrytvnbcrycrysngsc aaagataaaaggccgagtcggccagctccaagggtgtcacattcatct cag	
Combinatorial TCR _{A3} library flanking PCR	A3_flank_fwd	atcctgttaccaacagaccccaggacag	62
	A3_flank_rev	taggctctccatagagaccccccagccttacc	

rG = riboguanosine; +G = locked nucleic acid guanine; r = a, g; y = c, t; s = g, c; w = a, t; k = g, t; m = a, c; b = c, g, t; d = a, g, t; h = a, c, t; v = a, c, g; n = any base.